Flexible and Printed Electronics

Screen-printed, flexible, and eco-friendly thermoelectric touch sensors based on ethyl cellulose and graphite flakes inks

To cite this article: J Figueira *et al* 2023 *Flex. Print. Electron.* **8** 025001

Flexible and Printed Electronics

PAPER

Screen-printed, flexible, and eco-friendly thermoelectric touch sensors based on ethyl cellulose and graphite flakes inks

J Figueira[1,*], R M Bonito[1], J T Carvalho[1], E M F Vieira[2,3], C Gaspar[4], Joana Loureiro[1], J H Correia[2,3], E Fortunato[1], R Martins[1] and L Pereira[1,4]

[1] CENIMAT|i3N, Department of Materials Science, School of Science and Technology, NOVA University Lisbon and CEMOP/UNINOVA, Caparica, Portugal
[2] CMEMS-UMINHO, University of Minho, Campus Azurem, 4804-533 Guimaraes, Portugal
[3] LABBELS—Associate Laboratory, Braga, Guimarães, Portugal
[4] AlmaScience, Colab, Madan Parque, Caparica, Portugal
[*] Author to whom any correspondence should be addressed.

E-mail: joanarsfigueira@gmail.pt

Keywords: thermoelectric, touch sensors, ethyl cellulose, graphite, flexible substrates, screen-printing

Supplementary material for this article is available online

OPEN ACCESS

RECEIVED
5 October 2022

REVISED
10 February 2023

ACCEPTED FOR PUBLICATION
1 March 2023

PUBLISHED
18 April 2023

Abstract

Despite the undoubtable interest in energy conversion, thermoelectric (TE) materials can be approached from a temperature-sensitive perspective, as they can detect small thermal stimuli, such as a human touch or contact with cold/hot objects. This feature offers possibilities for different applications one of them being the integration with scalable and cost-effective, biocompatible, flexible, and lightweight thermal sensing solutions, exploring the combination of sustainable Seebeck coefficient-holding materials with printing techniques and flexible substrates. In this work, ethyl cellulose and graphite flakes inks were optimized to be used as functional material for flexible thermal touch sensors produced by screen-printing. Graphite concentrations of 10, 20 and 30 wt% were tested, with 1, 2 and 3 printed layers on four different substrates—office paper, sticker label paper, standard cotton, and organic cotton. The conjugation of these variables was assessed in terms of printability, sheet resistance and TE response. The best electrical-TE output combination is achieved by printing two layers of the ink with 20 wt% of graphite on an office paper substrate. Subsequently, thermal touch sensors with up to 48 TE elements were produced to increase the output voltage response (>4.5 mV) promoted by a gloved finger touch. Fast and repeatable touch recognition were obtained in optimized devices with a signal-to-noise ratio up to 340 and rise times bellow 0.5 s. The results evidence that the screen-printed graphite-based inks are highly suitable for flexible TE sensing applications.

1. Introduction

The thermoelectric (TE) phenomenon opens the door to green energy conversion and heat waste recovery, allowing the design and manufacturing of working devices with no noise, no vibrations, no moving parts nor gas emissions. This phenomenon is based on the Seebeck effect if the stimulus is a temperature gradient (ΔT) and the output is a voltage, or based on the Peltier effect, if considering the opposite stimuli/output combination. Unfortunately, these devices are usually associated with a low energy conversion efficiency, and the TE devices with better performances normally use toxic, rare, and expensive materials, which makes their commercial applications scarce. Furthermore, regular TE materials and devices are brittle, bulky and rigid [1].

The growing integration of sensors due to the increasing number of touch screen displays and devices boosts the global touch sensor market growth. Therefore, it is necessary to search for biocompatible, flexible, lightweight, and low-cost materials, and develop technologies compatible with low intensity stimuli, like low temperature (T) or low pressure. Moreover, the global TE generator market was valued at 472.5 million USD in 2020 and is projected to

reach more than 1440 million USD by 2030, growing at a compound annual growth rate of 11.8% [2]. Thus, there is a window of opportunity for TE materials research, not only for energy production but also for T sensing. Focusing on the last, printing technologies offer a potential route to produce sustainable TE devices at a lower price, in a large scale, and allowing a tailored architecture to meet the heat source stimulus requirements. A proof of that is the increasing number of publications that combine the topic of TE devices with wearable applications, flexible, organic, and printed materials [3]. Besides the possibility of flexibility and lightness, the TE sensors offer a good performance both for naked and glove covered fingers as they work with the ΔT formed between the finger and the device. This feature could be interesting in several situations, such as in industrial processes, patient-care activities, laboratory safety, among others, especially in a pandemic situation like the recent one we lived [4]. As a main advantage, over the existing touch sensors, a single TE element can not only distinguish a different finger T, but also sense and discriminate between fast and slow touches and give two symmetrical responses depending on the stimulated electrode, allowing for a Yes/No application [4].

Although these TE sensors do not have state-of-art fastest responses, specifically those related to the recovery of the 'off state', this set of features cannot be found in capacitive or resistive sensors, as they have different sensing mechanisms and responses and thus are not comparable.

A TE energy harvesting device is conventionally evaluated via TE figure of merit $ZT = S^2.\sigma.T.\kappa^{-1}$, where S is the Seebeck coefficient, σ stands for electrical conductivity, k denotes thermal conductivity and T is the medium measurement temperature. However, TE sensing capabilities are poorly compared via these indicators, because their performance is largely determined by the S of the active materials and the k of the full set of the device components [4, 5]. Thus, if using low k TE materials and substrates, as well as the integration of TE elements with little S in series, the production of TE sensors and detectors can be attained.

Graphite (G) among other carbon-based materials is known to have TE response but with relatively small S, when compared with more established TE materials [4]. However, there are reports showing that some of these materials can perform better than common organic conducting counterparts such as PEDOT:PSS, since the S is sometimes larger and they are able to sustain higher processing T if needed [6–11]. Moreover, when compared to carbon nanotubes and graphene, graphite is much cheaper [9], and has attracted the attention of several research groups [12–14]. Graphite ink is often used in printed electronics as a material for electrodes [15, 16], but reports of its use as a printed TE element in touch detection are limited. Regarding flexible and eco-friendly substrates, paper has been in focus for printed electronic applications, including in the fabrication of TE devices, due to its flexibility, abundance, and biodegradable nature [12, 17–21]. Meanwhile, fabrics have also been explored, with research being allocated to substrates like polyester [14, 22, 23], glassfiber fabric [24, 25], or cotton [26, 27] which has valuable properties for wearable and flexible applications, such as its breathability, foldability, and elastic recovery [28].

In terms of geometry, TE devices can assume vertical or planar structures, depending on how the heat flows and on the layout of the TE elements during fabrication [29], and can be made of thermocouples (p-n pairs) which is the common configuration or can be made with just one single TE type [4, 20, 30, 31]. The formulation of TE inks for screen-printing allows great freedom for different geometries and large area applications, without the need for complex cleanroom processes. Hence, in this work we show the possibility to combinate graphite flakes (G_{Flakes}) and ethyl cellulose (EC) for the development of low curing T inks for screen printing, to produce efficient flexible arrays of planar TE elements (single type) in paper and fabric substrates, fully printed and recyclable, in order to be used as thermal touch sensors. The main goal was to optimize the signal-to-noise ratio (SNR) of the sensor when stimulated with just one finger touch, promoting a ΔT along the samples.

2. Experimental

2.1. Materials

Ethyl cellulose (Sigma-Aldrich, extent of labeling: 48% ethoxyl) was dissolved in diacetone alcohol (DA) (4-Hydroxy-4methyl-2-pentanone 99% from Aldrich). Graphite Flakes (mesh 325, 99.8%, metal basis from Alfa Aesar®) were used as received. Commercial carbon screen paste (CRSN2644, from SunChemical®) and commercial aluminum foil were used to create the electrodes and conductive paths between the TE elements. Four different substrates were used: multi-function paper (office paper) with an 80 g m^{-2} grammage from Inapa Tecno; commercial thermal labels from Staples (referred to as sticker labels); organic cotton poplin fabric by Bo Weevil with a weight of 125–130 g m^{-2} and a 168-thread count, and natural cotton fabric from Fiacri.

2.2. Samples and devices preparation

2.2.1. Inks formulation and screen-printing

A screen-printing TE ink was produced, dissolving 5 wt% of EC in DA, with a stirring step of 300 rpm at 140 °C, and then adding three different concentrations of G_{Flakes}, 10, 20 and 30 wt%. The followed procedure to obtain these screen-printable inks is described in figure S1. The formulated TE inks

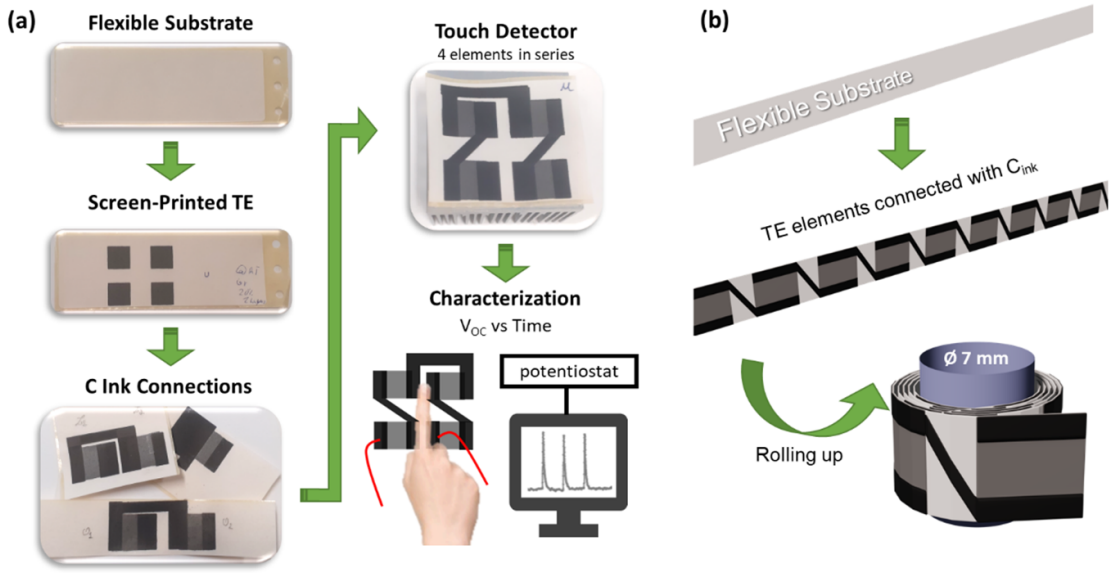

Figure 1. (a) Production steps to obtain a planar TE touch sensor, illustrating the example of a four-element sensor printed on a sticker label substrate and (b) 16-elements connected electrically in series and coiled around a cylindrical core.

were screen-printed using a mesh model 77–55 (mesh count 190, aperture 81 μm, thread diameter 55 μm), testing 1, 2 or 3 printed layers and varying the type of substrate—office paper, sticker label, cotton, and organic cotton. The TE elements were left to dry at room temperature (RT). Carbon paths between them were then printed with a mesh model 120–34 (mesh count 305, aperture 45 μm, and thread diameter 34 μm), and cured 30 min at 100 °C, using a hot plate. Schematic representations of the fabrication steps for the fully screen-printed TE touch sensors can be seen in figure 1(a), using the example of printing a four-element device on sticker label paper as substrate and in figure 1(b), where 16-elements connected electrically in series were printed, with an additional production step of coiling the printed films around a hollow core made with a piece of cardboard straw with a diameter of 7 mm.

2.2.2. Geometries

In figure S2 is shown an illustration of the printing patterns used to obtain the TE sensors. Firstly, the TE ink was printed followed by the carbon ink printing for electrical connections.

2.3. Characterization and testing

2.3.1. Substrates, inks, and samples characterization

A scanning electron microscope (SEM) Hitachi TM3030Plus tabletop workstation (Tokyo, Japan) was used to assess the printing quality of printed layers and substrate coverage. Since the substrates are insulators, an Iridium layer was deposited for better image acquisition.

The viscosity of the inks was measured using a viscometer CAP 2000+ (Brookfield Engineering), with a Spindle 09 (viscosity range: 20–10 800 cP), at a set T of 25 °C, at 5–10 rpm. The measured viscosity values were 1945 cP ± 9%, 3150 cP ± 14% and 10795 ± 25%, for 10 wt%, 20 wt% and 30 wt% G_{Flakes} ink, respectively. A screen-printable ink should have higher viscosities, typically between 1000–25 000 cP, when comparing with other printing techniques like inkjet or flexography [32, 33].

The Seebeck coefficients of the printed G/EC films were measured at RT, in a planar configuration using a homemade setup based on the 'two-probe' method [34]. This method consists in connecting one side of the film to a heated metal block at a fixed T (the block is heated by the application of successive voltage values, between 1 and 3 V) using the DC programmable source (Yokogawa model 7651) and the other side to a heat sink at RT, to generate ΔT along the film. This ΔT was measured using platinum wire resistors, Pt-100 (100 Ω at 0 °C precision resistor) at both metal blocks. The resulting thermovoltage (ΔV) was measured by an Agilent 34 410 A 61/2 Digit Multimeter. A linear plot of ΔV versus ΔT was expected, representative of a good thermal contact between the film and the blocks. The S values and corresponding errors were obtained using the LINEST function in an EXCEL worksheet. This function uses the least squares method to calculate the statistics for a straight line (that best fits the experimental data) and returns an array of parameters describing that line, including S (from the slope of the linear fitting), and the associated error.

The sheet resistance (R_{Sheet}) was measured with a Biorad/Nanometrics HL5500 Hall effect system, using van der Pauw contact geometry. The samples were cut in quadrangular shapes and covered with Ag

ink at the corners. The measurements were conducted at RT (temperature kept between 22.5 °C–23.1 °C) at a relative humidity (RH) of 38% and 46% for the organic cotton and cotton substrates, respectively. Regarding the paper substrates the RT was kept between 22.7 °C and 23.1 °C, while the RH was 40% and 44% for office paper and the sticker label substrates, respectively.

2.3.2. Devices characterization

The TE sensors response to touch events was obtained using a Gamry Instruments Reference 600 Potentiostat in a configuration where the open circuit potential (V_{OC}) was measured over time, while touching (or not) the sample with the gloved finger. The time step for data acquisition was fixed at 0.1 s in every measurement. To perform the characterization of the sensors on the potentiostat, two electrodes of carbon ink (C_{ink}) were screen-printed in opposite sides of the quadrangular TE elements and aluminum foils were added (gluing them to the C_{ink} zones) to extend the devices electrical contacts. To test the scalability of the process, the C_{ink} was also used to connect the elements between them. Mechanical stress tests were performed by bending the sensors with controlled curvature radii (7, 15 and 25 mm) and measuring its response over time (up to 800 h).

3. Results and discussion

The TE inks were printed on four different substrates: (i) cotton (Cot), (ii) organic cotton (OrgCot), (iii) office paper (OP) and (iv) sticker label paper (SL). It is assumed that each substrate has a characteristic k that would interfere with the response time of the sensors and other distinctive properties that would vary the ink's adhesion and printed layers quality, which consequently will lead to different sensor responses. For instance, the two chosen fabrics show a difference in the mesh apertures and the two papers show differences in the fiber's diameters and binder compounds. Likewise, depending on the wt% of G_{Flakes} and number of printed layers, the printability of the inks, as well as the electrical and TE properties of the films differ. Besides the chosen materials and printing conditions, the architecture adopted to fabricate the touch sensors is also very important, not only in terms of the number of connected elements, but also in terms of heat collection and thermal stabilization towards the increment of the maximum ON state voltage (V_{ON}).

3.1. Electrical and morphological characterization

3.1.1. Cotton and organic cotton substrates

Figure 2 presents the average of the measured R_{Sheet} values, considering different combinations of variables (10–30 wt% G_{Flakes} and 1 to 3 printed layers), for both fabric substrates. As expected, the measurements show that increasing G_{Flakes} wt% in the ink results in a higher electrical conductivity for the printed elements. In addition, regardless of the substrate, it is possible to conclude that R_{Sheet} values of the samples are also reduced with the number of printed layers. This happens due to a better substrate coverage, increasing the percolation between the conductive flaked particles.

Comparing the two fabric substrates, the films printed on OrgCot have always higher R_{Sheet} values, as well as higher associated errors, independently of the studied conditions, which means that Cot allows better and more repeatable results. The SEM images (figure 3) help to understand how the fabric woven structure affects the printability and coverage of both fabric substrates. The first image of each set of figures 3(a) and (b) presents the substrates before coating while the ensuing images are for different printing conditions and inks formulations (the extreme conditions, one layer of 10 wt% vs three layers of 30 wt%, and a combination in between, two layers of 20 wt%).

For the condition of three printed layers of the 30 wt% G_{Flakes} ink it is observed a uniform coverage of the surface on the Cot substrate, barely leaving any thread or hole exposed, while in the OrgCot substrate the fabric threads are easily identified and spotted. This can be due to different factors such as fiber staple length, weaving method, number of twisted fibers, degree of twisting or fiber treatment, leading to a lower printing quality [35, 36]. Although OrgCot initially appears to have a more closed mesh and a smoother surface, the Cot substrate promotes a better ink adhesion and G_{Flakes} assembling, increasing the layer uniformity and a more efficient formation of electrical paths, which matches their R_{sheet} values, that have the lowest value for three layers of 30 wt% of $270 \pm 24\ \Omega\ sq^{-1}$ and $831 \pm 55\ \Omega\ sq^{-1}$, for Cot and OrgCot, respectively.

3.1.2. Office paper and sticker label

Similar conditions were implemented to paper substrates and used for comparison with fabric substrates. The R_{Sheet} was measured on samples with 1–3 layers combined with G_{Flakes} concentrations of 10, 20 and 30 wt% (figure 4). Similarly, to what was observed for the fabric substrates the increase in the number of layers and G_{Flakes} wt% lead to a decrease of the R_{Sheet} values of the printed sensing elements. For paper substrates the observed R_{Sheet} values are not distinctive, probably due to the fact that they are alike in terms of roughness, porosity and fiber distribution.

The SEM images in figures 5(a) and (b) show clear differences in the surface topography when compared to the printed fabrics (figure 3). It shows an highly efficient fiber covering, from one printed layer, resulting in an immediate electrical percolation. Thus, the ink saturation is more prevalent in paper substrates which can be explained by the fiber ink absorption

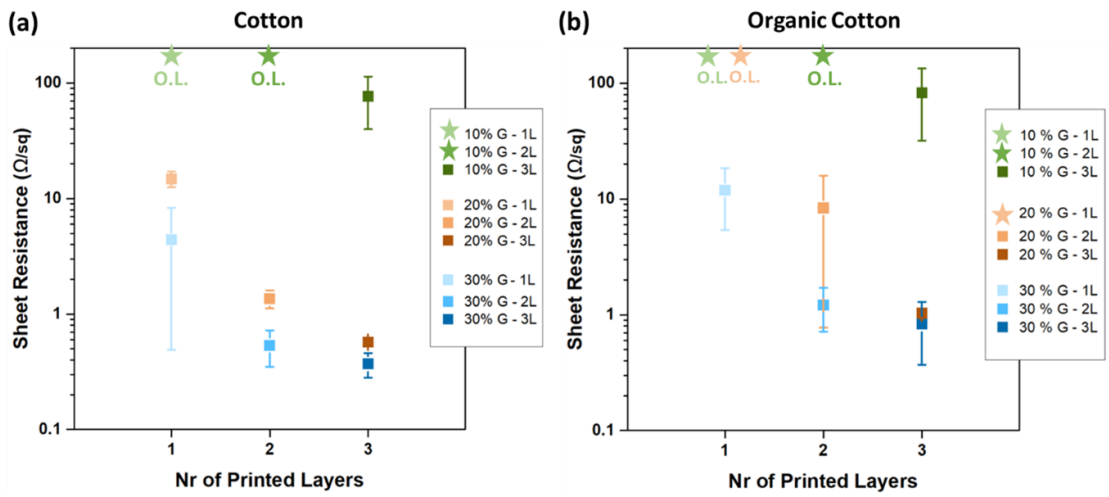

Figure 2. Average R_{Sheet} values for different number of printed layers (1–3 layers) and graphite wt % composition (10% to 30%) on: (a) cotton, and (b) organic cotton substrates.

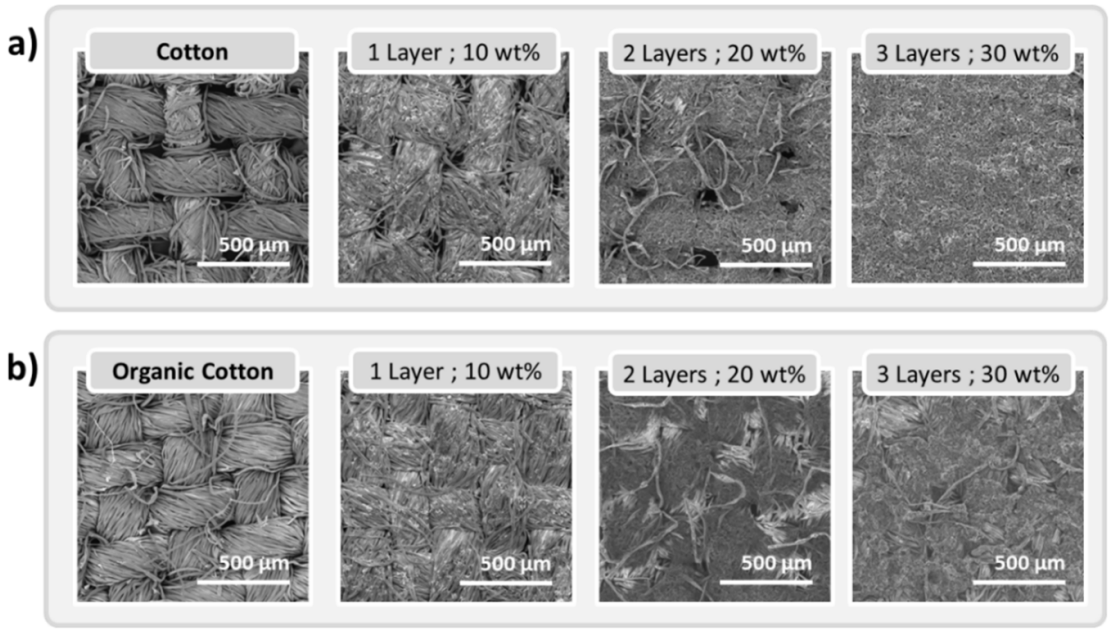

Figure 3. Surface SEM images of screen-printed TE films on: (a) cotton, and (b) organic cotton substrates. For comparison purposes, the first image of each set presents both fabric substrates without TE material.

as well as the production method of the fabric substrates, that undergo a weaving process leading to higher apertures in between the threads, hence more porous, whereas in the paper fibers, the porous size is significantly smaller and the fibers are more randomly compressed. The ink uptake of the substrate is then controlled by the porosity and fiber absorption, making the fabric substrates better candidates for ink absorption, thus lower layer saturation and less ink consumption. In the extreme condition of three layers of 30 wt%, it is noticeable an excess in G_{Flakes} ink on the paper substrates, resulting in a common screen-printing defect where the printed layer surface showcases the mesh aperture, like small dots. Although this translates into a rougher surface and ink waste, the R_{Sheet} presents its lowest values of $364 \pm 20\ \Omega\ sq^{-1}$ and $467 \pm 33\ \Omega\ sq^{-1}$ for OP and SL, respectively.

3.2. Touch detection tests

The electrical and morphological characterization indicated Cot and OP as the prime printing substrate options and the clear influence of the number of printed layers and G_{Flakes} wt%. Combining both aspects, the optimal conditions for both substrates are three printed layers of 30 wt% ink. However, aiming a reduced device processing time and less expense of the active material amount, as well as a higher flexibility, the option of two layers of 20 wt% ink was also addressed on OP (R_{Sheet} of $751 \pm 20\ \Omega\ sq^{-1}$) to produce some of the final touch sensors.

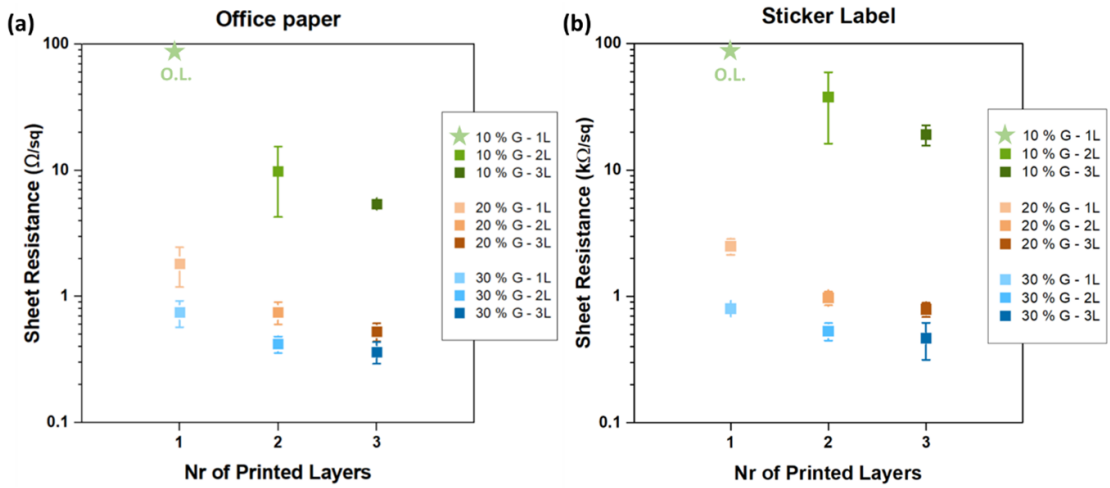

Figure 4. Average sheet resistance values for each number of printed layers (1–3 layers) and graphite wt% composition (10% to 30%), on: (a) office paper, and (b) sticker label substrates.

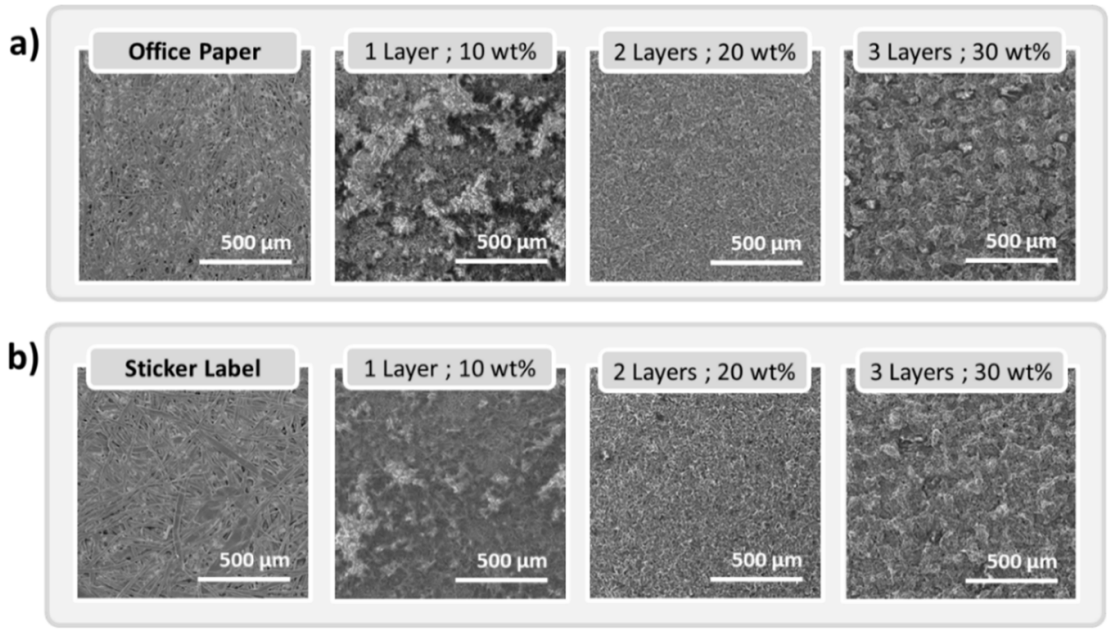

Figure 5. Surface SEM images of screen-printed TE films on: (a) office paper, and (b) sticker label substrates. For comparison purposes, the first image of each set presents both fabric substrates without TE material.

To complement the characterization of the samples printed on OP and Cot, S measurements were performed (S3). As expected [4, 7], all values were positive (G is reported as a p-type material) and around 20 μV/°C, regardless of the substrate and printing conditions (Figure 6), meaning that the TE behaviour for this specific application will show similar responses notwithstanding the differences in R_{Sheet}. The V_{OC} of the samples was measured over time, in order to study the gloved finger touches response of the TE elements. The V_{ON} is the V_{OC} when the sample is experiencing a ΔT due to a finger touch while V_{OFF} is the V_{OC} when there is no ΔT. At the beginning of each test, the sample was measured at least 30 s with no ΔT applied to acquire a baseline. After this stabilization time, the stimulation of the sensors began, and the V_{OC} was left to reset to its initial value between touches.

3.2.1. Cotton sensors with different number of elements

Figure 7(a) exhibits the positive and negative V_{OC} peaks, which correspond touches (around 2 s) on each of the sensor positive and negative terminal, respectively, where the same sensor can generate two different responses. When TE materials are exposed to a ΔT the majority carriers move from the hot side to the cold side, originating an electrical response, hence the carrier movement will also invert when

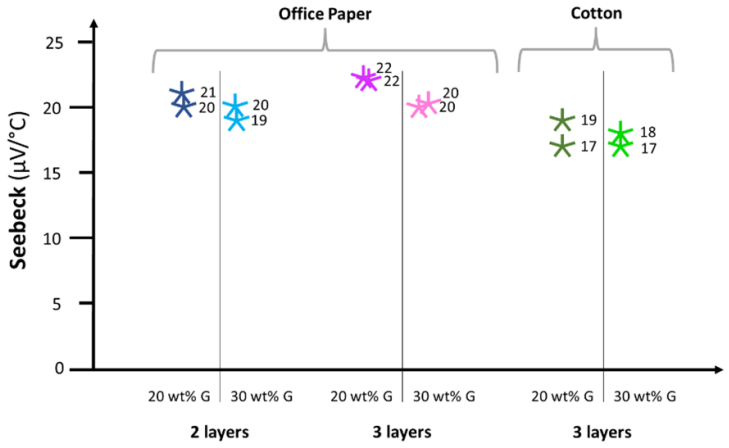

Figure 6. Seebeck coefficient measurement results for different printing conditions using OP and Cot substrates.

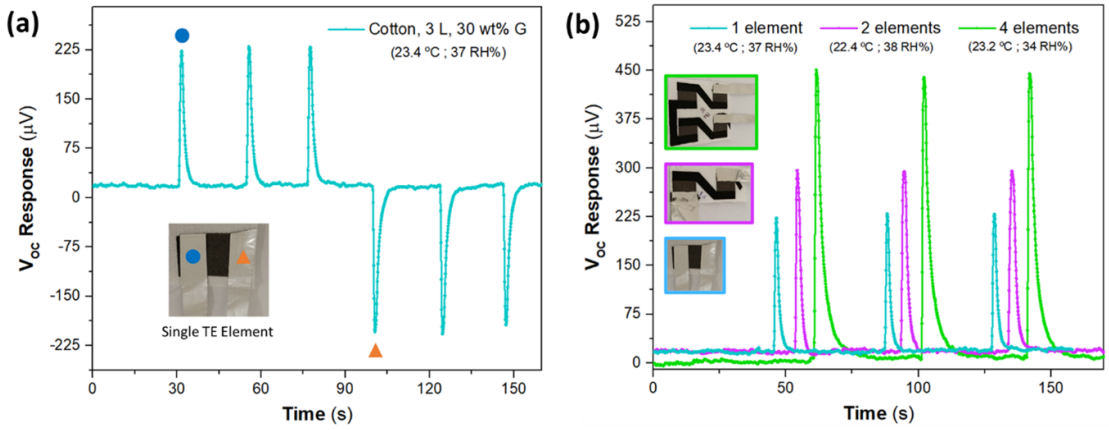

Figure 7. (a) Gloved finger touch test for a Yes or No response based on symmetric ΔT—the first three peaks were obtained when touching the left electrode and the last three peaks when touching the right electrode and b) Comparison of the TE response for touch sensors printed on cotton with 1, 2 and 4 elements connected electrically in series—3 layers, and 30 wt% G_{Flakes}.

there is an inversion of the said gradient. This behavior can be used for a Yes or No application, depending on which side the user touches the sensor.

Figure 7(b) shows the V_{OC} increase when connecting elements electrically in series, using 1, 2 and 4 elements. The used geometries are shown in the inset images, and the corresponding SNR values, voltage amplitudes (V_{AMP}) and rise/fall times (T_{Rise} and T_{Fall}, respectively) can be found in table 1. The SNR parameter of a sensor relates the signal amplitude to the background noise (measuring V_{OFF} over time) and its values are determined by $(V_{ON} - V_{OFF})/\text{stdev}(V_{OFF})$ [4].

When increasing the number of elements, it increases the SNR value, since the maximum V_{ON} increases, due to the S sum, while the noise remains similar for the three cases. Data shows that all tested geometries have a noticeable output voltage when thermally stimulated (touch ~2 s) and could be used as touch sensor with reproducible V_{OC} responses.

The V_{AMP} values scales with the increasing number of TE elements in the sensor. In theory [2], when adding in series equal TE elements consisting of p-n junctions, the sum of each element's S value, as well as its electrical resistance, will lead to a proportional increase in V_{AMP}. Nevertheless, our printed sensors, unlike regular TE devices, have single type TE elements, and the observed behavior is not the same. The C_{ink} used to connect different elements is responsible for the electrons diffusion from hot to cold regions and this is why our carbon paths are diagonal across the sensor. Since C_{ink} has small S and is p-type, there is a loss in the yield and efficiency of the sensor, escalating with the insertion of more elements. Ideally, using n-type electrical connections between sensing elements instead would overcome this issue. Furthermore, it is important to consider that the geometry of the serialized elements still needs optimization: firstly, the often-long carbon tracks printed onto an insulator substrate offer additional resistance to the sensor; secondly, as the number of elements increases

Table 1. Average values of the SNR, V_{AMP}, T_{Rise}, and T_{Fall} for the peaks in figure 7(b).

Number of TE elements	SNR	V_{AMP} (μV)	Rise time (s)	Fall time (s)
1	162 ± 11	209 ± 4	0.63 ± 0.01	4.3 ± 0.5
2	205 ± 50	277 ± 1	0.73 ± 0.23	3.6 ± 0.6
4	244 ± 30	439 ± 10	0.51 ± 0.01	6.2 ± 0.1

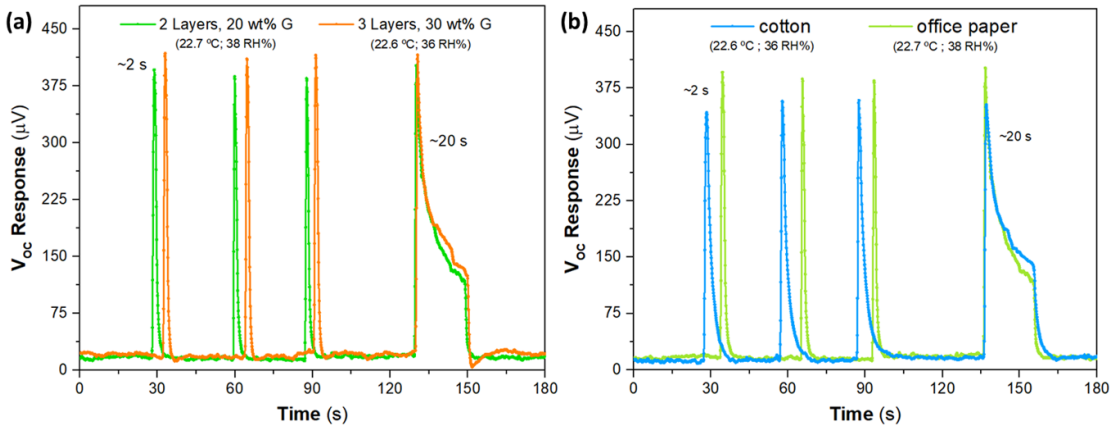

Figure 8. (a) Comparison of four-element touch sensors printed on office paper with two layers of 20 wt%, and three layers of 30 wt%, and (b) four-element touch sensors with two layers of 20 wt%, printed on office paper and cotton, for comparison of substrates.

Table 2. Average values of the SNR, V_{AMP}, T_{Rise} and T_{Fall} for the four-element paper sensors printed with different conditions (figure 10(a)) and for sensors printed with two layers of 20 wt% of G, in different substrates (figure 10(b)).

Substrates	Conditions	SNR	V_{AMP} (μV)	Rise time (s)	Fall time (s)
Office paper	Two Layers, 20 wt%	340 ± 51	374 ± 4	0.40 ± 0.12	1.82 ± 0.07
	Three Layers, 30 wt%	295 ± 73	396 ± 3	0.46 ± 0.03	1.36 ± 0.09
Cotton	Two Layers, 20 wt%	326 ± 36	341 ± 9	0.56 ± 0.06	5.67 ± 0.74
Office paper		322 ± 106	374 ± 5	0.47 ± 0.12	1.85 ± 0.06

it becomes more difficult for the finger to touch all the elements uniformly.

The response time is characterized by T_{Rise} and T_{Fall} values, which were obtained by normalizing the curves and measuring the time needed for the voltage to increase from 10%–90% and to decrease from 90 to 10%, respectively [37]. It is observed that the number of elements does not appear to influence the T_{Rise} significantly. However, when it comes to T_{Fall} values, there is a slight decrease when adding sensing elements. We attribute this also to the non-uniform stimulation of the sensing elements that will generate differences in ΔT established between the hot and cold side.

3.2.2. Cotton and office paper sensors with different conditions

Although the initial touch detection tests were performed using the optimal conditions of three printed layers of the ink with 30 wt% of G_{Flakes}, a comparison of sensors with different ink formulations and printing conditions was made using OP as substrate, figure 8(a). Three faster touches were performed (~2 s) followed by a longer touch (~20 s) to evaluate the V_{OC} and T_{Fall} behaviors for the different sensors.

In general, less resistive TE elements are obtained when increasing the number printed layers and increasing the G_{Flakes} wt% in inks formulations. Nonetheless, when comparing the SNR values and response times (table 2) of two printed layers with 20 wt% of G_{Flakes} and three printed layers with 30 wt% of G_{Flakes}, it does not justify using more material to produce each sensor, since the S values are similar (figure 7). Therefore, in order to save material and have a faster process, the condition of two printed layers with 20 wt% of G_{Flakes} was chosen to perform a test comparing the Cot and OP substrates, figure 8(b).

Furthermore, it is expected that the inks with more G content have higher k, interfering with the response speed in apparently higher V_{AMP} value. However, for longer touch time and considering the experimental errors introduced by the manual test and possible variation in RT, the difference in the signal is not significant. Thus, the performance of four-element sensors printed on OP and Cot using two layers with 20 wt% of G_{Flakes} was compared (figure 8(b)). Table 2 presents the SNR, V_{AMP}, T_{Rise} and T_{Fall} values

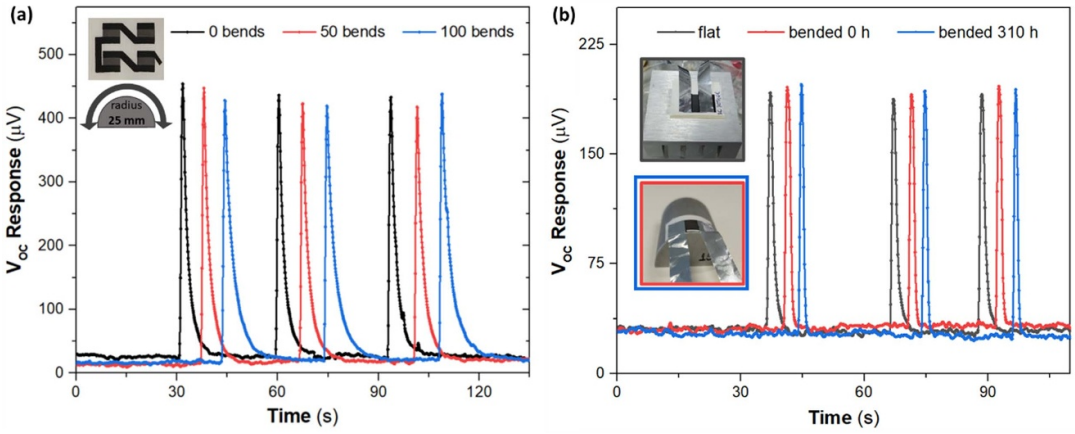

Figure 9. (a) Results for a dynamic bending test using a cylinder with 25 mm of curvature radius, with a four-element sample printed on cotton (three layers, 30 wt% G_{Flakes}), and (b) Static bending test for a single element touch sensor using a sticker label substrate—three layers of 30 wt% G_{Flakes}.

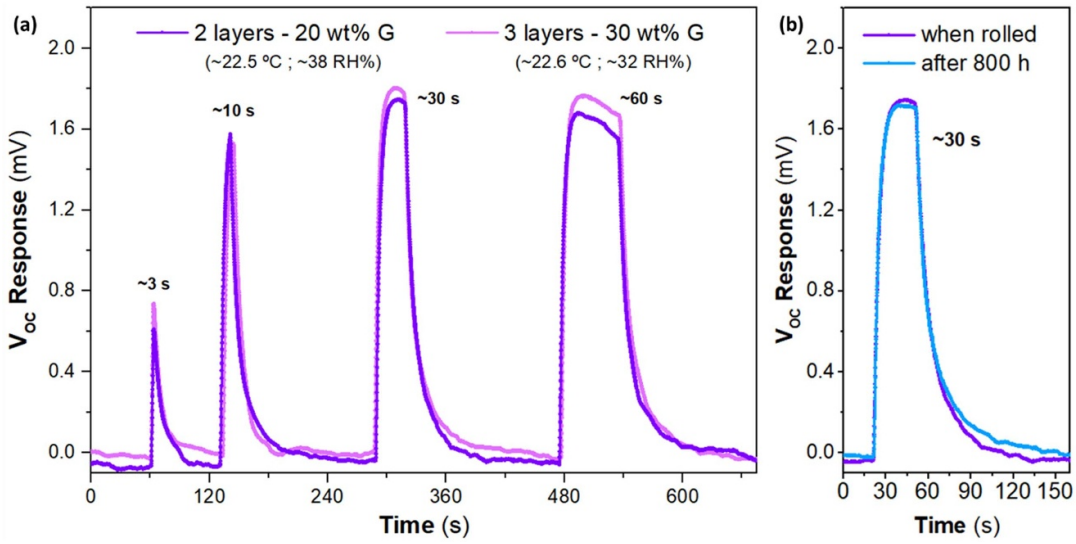

Figure 10. Comparison of 16-elements connected electrically in series, printed on paper with different conditions, (a) the dark purple curve is of a sample with two printed layers of 20 wt% G_{Flakes}, and the light purple is of a sample with three layers of 30 wt% G_{Flakes}, and (b) the sample in dark purple being remeasured after 800 h rolled up.

for those samples indicating that the OP substrate is better than Cot, both in terms of V_{AMP} and in terms of response times. The response speed is related to the k of the TE film/substrate combination, and it is expected that cotton shows a higher thermal resistance, both in absorbing the thermal stimuli and in freeing it back to the environment, since it is thicker than paper and has patterned apertures along the material.

3.2.3. Bending and durability

A mechanical bending test was performed to evaluate the endurance of the thermal touch sensor printed with three layers of 30 wt% G, on cotton substrate. These printing conditions were chosen assuming that for thicker films and higher amounts of printed material the impacts of the cyclic bending tests would be magnified, inducing more surface defects, and reducing the performance of the sensor. The four-element sample was measured before any bending effort and after 50 (red curve) and 100 (blue curve) bending cycles, as can be seen in figure 9(a). Although the recovery time and the electrical resistances increase with the bending stress, we can see that the sensor endured after the 100 bending cycles, maintaining its response.

A single element sensor printed on sticker label substrate, with three layers and 30 wt% G, was tested over a longer bending period of 310 h, continuously, with a smaller curvature radius of 15 mm, figure 9(b). The results indicated that the sensor's performance was not affected over this mechanical bending test and this type of sensors can be used in flexible applications.

A series of 16 TE elements were printed and connected to evaluate if it is possible to increase the

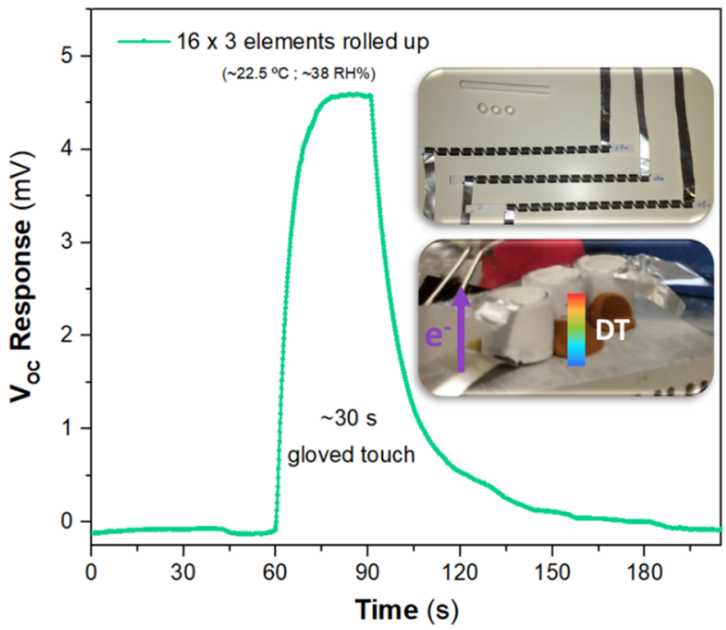

Figure 11. Voltage response (V_{OC}) of three rolled arrays of 16 TE elements, totaling 48 elements connected electrically in series, printed on office paper, with two layers and 20 wt% G_{Flakes}.

SNR values, due to the V_{AMP} increase. The devices were rolled around a hollow cylindric shape as core, a piece of cardboard straw with 7 mm of diameter (figure 1(b)), to facilitate the heat collection from a single finger touch, figure 10. Figure 10(a) shows the comparison of output response of sensors printed on OP with different conditions (two layers of 20 wt% of G_{Flakes} vs three layers of 30 wt% of G_{Flakes}) for different touch durations. Figure 10(b) shows the results for the sample printed with two layers and 20 wt% G_{Flakes}, after being rolled up for 800 h and stored in a non-vacuum environment. The graphic indicates that the differences between the samples are not significant and the bendability and durability of the sensors is demonstrated.

For the final proof-of-concept of output signal improvement, 48 elements were connected electrically in series (3 × 16 elements arrays), using OP as substrate (figure 11). With this planar-vertical configuration, the response for one gloved finger touch was maximized, surpassing 4.5 mV.

4. Conclusions

The design, production, and optimization of touch sensors based on G_{Flakes}/EC screen-printable inks are demonstrated in this work. We achieved flexible, lightweight, and low-cost TE devices, for low-T applications, using eco-friendly materials and processes. The optimization of these devices involved the choice of the ideal ink formulation, printing conditions and substrate set, and the adequate architecture/geometry for the determined application—detect human gloved touches.

The 10 wt% G_{Flakes} ink originates more resistive TE elements, while the 30 wt% ink is less adequate to print a large number of elements and layers. Due to its high viscosity, manual screen-printing is more challenging. The ideal printing conditions were found to be two printed layers with 20 wt% of G_{Flakes} since they allow the saving of material and a faster production process. Although three printed layers with 30 wt% are more electrically conductive, for this application the performances showed to be similar. Comparing the printed substrates, the most suited for this type of applications were office paper and cotton, as they provide better surface coverage, lower R_{Sheet}, and higher SNR value, where office paper gave higher and faster responses.

The bending tests showed that the sensors performance was not affected over the mechanical stress, revealing a high flexibility with curvature radii down to 7 mm. Indeed, it was demonstrated that with sensors with up to 48 elements rolled up, it was possible to reach more than 4.5 mV of output voltage response. However, for fast and repeatable touch recognition, the best choice suggests less elements, where response times bellow half a second can be achieved.

Depending on the application, different combinations of TE elements can be designed and printed, using compatible and up-scalable R2R technologies.

Data availability statement

All data that support the findings of this study are included within the article (and any supplementary files).

Acknowledgments

This work was financed by national funds from FCT—Fundação para a Ciência e a Tecnologia, I P, in the scope of the projects LA/P/0037/2020, UIDP/50025/2020, and UIDB/50025/2020 of the As-sociate Laboratory Institute of Nanostructures, Nanomodelling and Nanofabrication—i3N, and by projects PTDC/NAN-MAT/32558/2017 and PTDC/CTM-PAM/4241/2020. E V thanks the FCT—Fundação para a Ciência e a Tecnologia, I P, under the national support to R&D units Grant, through the reference project UIDB/04436/2020 and UIDP/04436/2020. J F and J T C thank the support from FCT—Fundação para a Ciência e a Tecnologia, I P through the PhD scholarships SFRH/BD/121679/2016 and SFRH/BD/139225/2018, respectively. This work has received funding from the European Union Horizon 2020 Research and Innovation Programme under the Grant Agreements Nos: 640598 (ERC-2014-STG NEW-FUN), 952169 (SYNERGY, H2020-WIDESPREAD-2020-5, CSA), and 101008701 (EMERGE, H2020-INFRAIA-2020-1). The authors would like to thank Miguel Alexandre for some explanatory illustrations.

ORCID iDs

J Figueira https://orcid.org/0000-0002-5996-9831
J T Carvalho https://orcid.org/0000-0002-6654-8859
E M F Vieira https://orcid.org/0000-0001-8198-6024
Joana Loureiro https://orcid.org/0000-0001-9926-4898
E Fortunato https://orcid.org/0000-0002-4202-7047
R Martins https://orcid.org/0000-0002-1997-7669
L Pereira https://orcid.org/0000-0001-8281-8663

References

[1] Urban J J, Menon A K, Tian Z, Jain A and Hippalgaonkar K 2019 New horizons in thermoelectric materials : correlated electrons, organic transport, machine learning, and more *J. Appl. Phys.* **125** 180902
[2] Zhu S, Fan Z, Feng B, Shi R, Jiang Z, Peng Y, Gao J, Miao L and Koumoto K 2022 Review on wearable thermoelectric generators: from devices to applications *Energies* **15** 3375
[3] Advanced Search Query Builder (available at: https://www.webofscience.com/wos/woscc/advanced-search)
[4] Figueira J, Loureiro J, Vieira E, Fortunato E, Martins R and Pereira L 2021 Flexible, scalable, and efficient thermoelectric touch detector based on PDMS and graphite flakes *Flex. Print. Electron.* **6** 045018
[5] Koskinen T, Juntunen T and Tittonen I 2020 Large-area thermal distribution sensor based on multilayer graphene ink *Sensors* **20** 5188
[6] Tran V and Volz S 2018 High thermoelectric performance of graphite nanofibers *Nanoscale* **8** 3784–91
[7] Correia A R 2019 Tailoring carbon-based materials for thermoelectric application (Universidade do Porto) (https://doi.org/10.1002/cap.10072)
[8] Phillips C, Al-Ahmadi A, Potts S-J, Claypole T and Deganello D 2017 The effect of graphite and carbon black ratios on conductive ink performance *J. Mater. Sci.* **52** 9520–30
[9] Du Y, Li H, Jia X, Dou Y, Xu J and Eklund P 2018 Preparation and thermoelectric properties of graphite/poly(3,4-ethyenedioxythiophene) Nanocomposites pp 4–12
[10] Zhang Y, Heo Y, Park M and Park S 2019 Recent advances in organic thermoelectric materials : principle mechanisms and emerging carbon-based green energy materials *Polymers* **11**
[11] Lee Y M, Lim A, Park R and Kim H 2018 High-performance thermoelectric bracelet based on carbon nanotube ink printed directly onto a flexible cable † *J. Mater. Chem.* A **6** 19727–34
[12] Mulla R, Jones D R and Dunnill C W 2020 Thermoelectric paper : graphite pencil traces on paper to fabricate a thermoelectric generator *Adv. Mater. Technol.* **5** 2000227
[13] Rademann P K, Klaus S, Chem P, Phys C, Andrei V, Bethke K and Rademann K 2016 As featured in : copper (I) oxide—graphite—polymer pastes and the applications of such flexible composites † *Phys. Chem. Chem. Phys.* 10700–7
[14] Du Y, Xu J, Wang Y and Lin T 2017 Thermoelectric properties of graphite-PEDOT : PSS coated flexible polyester fabrics *J. Mater. Sci. Mater. Electron.* **28** 5796–801
[15] Emani H R K M, Zhang X, Wang G, Maddipatla D, Saeed T, Wu Q, Lu W and Atashbar M Z 2021 Development of a screen-printed flexible porous graphite electrode for Li-ion battery *2021 IEEE Int. Conf. on Flexible and Printable Sensors and Systems (FLEPS)* pp 1–4
[16] Kadara R O, Jenkinson N, Li B, Church K H and Banks C E 2008 Manufacturing electrochemical platforms : direct-write dispensing versus screen printing *Electrochem. Commun.* **10** 1517–9
[17] Ling H, Chen R, Huang Q, Shen F, Wang Y and Wang X 2020 Transparent, flexible and recyclable nanopaper-based touch sensors fabricated via inkjet-printing *Green Chem.* **22** 3208–15
[18] Kanaparthi S and Badhulika S 2017 Low cost, flexible and biodegradable touch sensor fabricated by solvent-free processing of graphite on cellulose paper *Sensors Actuators* B **242** 857–64
[19] Rojas J P, Conchouso D, Arevalo A, Singh D, Foulds I G and Hussain M M 2017 Paper-based origami flexible and foldable thermoelectric nanogenerator *Nano Energy* **31** 296–301
[20] Andersson H, Šuly P, Thungström G, Engholm M, Zhang R, Mašlík J and Olin H 2019 PEDOT: PSS thermoelectric generators printed on paper substrates *J. Low Power Electron. Appl.* **9** 14
[21] Dong Z, Liu H, Yang X, Fan J, Bi H, Wang C, Zhang Y and Luo C 2021 Facile fabrication of paper-based flexible thermoelectric generator *npj Flex. Electron.* **5** 0–5
[22] Jung M, Jeon S and Bae J 2018 Scalable and facile synthesis of stretchable thermoelectric fabric for wearable self-powered temperature sensors † *RSC Adv.* **8** 39992–9
[23] Kim M K and Kim M S 2013 Wearable thermoelectric generator for human clothing applications *Transducers 2013 (Barcelona, Spain, 16–20 June 2013)* pp 1376–9
[24] Shin S *et al* 2017 High-performance screen-printed thermoelectric films on fabrics *Sci. Rep.* **7** 1–9
[25] Kim S J, We J H and Cho B J 2014 A wearable thermoelectric generator fabricated on a glass fabric *Energy Environ. Sci.* **7** 1959
[26] Karttunen A J, Sarnes L, Townsend R, Mikkonen J and Karppinen M 2017 Flexible thermoelectric ZnO–organic superlattices on cotton textile substrates by ALD/MLD *Adv. Electron. Mater.* **3** 1600459
[27] Paleo A J, Vieira E M F, Wan K, Bondarchuk O, Cerqueira M F, Bilotti E, Melle-Franco M and Rocha A M 2020 Vapor grown carbon nanofiber based cotton fabrics with negative thermoelectric power *Cellulose* **27** 9091–104

[28] Hosseini Ravandi S A and Valizadeh M 2011 Properties of fibers and fabrics that contribute to human comfort *Improving Comfort in Clothing* 61–78
[29] Glatz W, Schwyter E, Durrer L and Hierold C 2009 Bi_2Te_3-based flexible micro thermoelectric generator with optimized design *J. Microelectromech. Syst.* **18** 763–72
[30] Søndergaard R R, Hösel M, Espinosa N, Jørgensen M and Krebs F C 2013 Practical evaluation of organic polymer thermoelectrics by large-area R2R processing on flexible substrates *Energy Sci. Eng.* **1** 81–88
[31] Burton M R, Mehraban S, Beynon D, McGettrick J, Watson T, Lavery N P and Carnie M J 2019 3D printed SnSe thermoelectric generators with high figure of merit *Adv. Energy Mater.* **9** 1900201
[32] Cao Z 2014 Printable thermoelectric devices for energy harvesting (faculty of physical science and engineering) *PhD Thesis* University of Southampton
[33] Öhlund T 2014 Metal films for printed electronics : ink-substrate interactions and sintering *PhD Thesis* Mid Sweden University
[34] Vieira E M F, Silva J P B, Veltruská K, Matolin V, Pires A L, Pereira A M, Gomes M J M and Goncalves L M 2019 Highly sensitive thermoelectric touch sensor based on p-type SnOx thin film *Nanotechnology* **30** 435502
[35] Angelova R A 2019 Organic cotton: technological and environmental aspects *23rd Int. Scientific Conf. FPEPM 2018* pp 351–6
[36] Atalie D, Ferede A and Rotich G K 2019 Effect of weft yarn twist level on mechanical and sensorial comfort of 100% woven cotton fabrics *Fash. Text* **6** 1–12
[37] Figueira J, Gaspar C, Carvalho T, Loureiro J, Fortunato E and Martins R 2019 Sustainable fully printed UV sensors on cork using zinc oxide/ethylcellulose inks *Micromachines* **10** 601